AIVP ADVANCES IN IMAGE AND VIDEO PROCESSING
SOCIETY FOR SCIENCE AND EDUCATION UNITED KINGDOM

On Supervised Methods for Segmentation of Blood Vessels in Ocular Fundus Images

Edward James, Antonio Francisco
School of Informatics and Computing, Indiana University Bloomington, USA;
Edward.james85@gmail.com, antonio.francisco01@gmail.com

ABSTRACT

Information about the retinal blood vessel network is important for diagnosis, treatment, screening, evaluation and the clinical study of many diseases such as diabetes, hypertension and arteriosclerosis. Automated segmentation and identification of retinal image structures had become one of the major research subjects in the fundus imaging and diagnostic ophthalmology. Automatic segmentation of blood vessels from retinal images is considered as first step in development of automated system for ophthalmic diagnosis. With the development of computational efficiency, the pattern classification and image processing techniques are increasingly used in all fields of medical sciences particularly in ophthalmology. In this paper, we have presented a review of supervised classification algorithms for retinal vessel segmentation available in the literature. We outline the principles upon which retinal vessel segmentation algorithms are based. We discuss current supervised classification techniques used to automatically detect the blood vessels.

Keywords: Image segmentation, Pattern Recognition, Supervised classification, Ocular Fundus, Retinal image analysis.

1. INTRODUCTIN

The eye is a unique region of the human body where the vascular condition can be directly observed in-vivo. By using an ophthalmoscope to look through the pupil, a magnified image of the retina and blood vessels can be observed that course across its anterior surface [1]. The blood vessels appear as elongated features in retinal images that are of different intensity than the background, and their thickness is always smaller than a certain value. They enter into the retina by the optic disc and form branches of vessels that are connected.

Information about the retinal vascular network is important for diagnosis, treatment, screening, evaluation and the clinical study of many diseases such as diabetes, hypertension

and arteriosclerosis [2]. Several eye diseases such as retinal artery occlusion and chorodial neovascularization [3] induce changes in the retinal vascular network [4]. Blood vessels are the most predominant and stable structures appearing in the ocular fundus, therefore reliable vessel extraction is a prerequisite for subsequent retinal image analysis and processing. Some of the main clinical objectives reported in the literature for retinal vessel segmentation are the implementation of screening programs for diabetic retinopathy [4, 5] evaluation of retinopathy of prematurity [6], foveal avascular region detection [7], arteriolar narrowing [8, 9], the relationship between vessel tortuosity and hypertensive retinopathy [10], vessel diameter measurement to diagnose cardiovascular diseases and hypertension [11, 12], and computer-assisted laser surgery [2, 13]. Other indirect applications include automatic generation of retinal maps for the treatment of age-related macular degeneration [14]; extraction of characteristic points of the retinal vasculature for temporal or multimodal image registration [15, 16]; retinal image mosaic synthesis [17]; identification of the optic disc position [18, 19], and localization of the fovea [20]; change detection [6, 21-23] and tracking in video sequences [24, 25]. All these techniques depend on vessel extraction. The network of retinal vessels is distinctive enough to each individual and can be used for biometric identification, although it has not yet been extensively explored [26]. Furthermore, the segmentation of the vascular tree seems to be the most appropriate representation for the image registration applications due to three of the following reasons: 1) it maps the whole retina; 2) it does not move except in a few diseases; 3) it contains enough information for the localization of some anchor points. Mostly vascular branching and crossover points are used as landmark features [27].

The quantification of vessel features, such as length, width and branching pattern, among others, can provide new insights to diagnose and stage pathologies which affect the morphological and functional characteristics of blood vessels. However, when the vascular network is complex, or the number of images is large, manual measurements can become tiresome or even impossible. A feasible solution is the use of automated analysis, which is nowadays commonly accepted by the medical community.

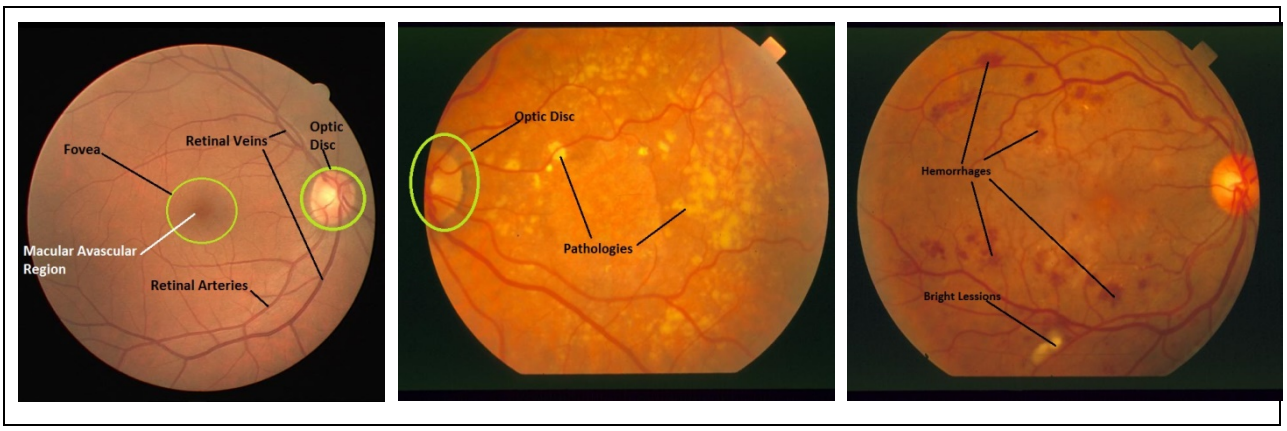

Figure 1: Anatomical Structures in Retinal Images

2. RETINAL BLOOD VESSELS MORPHOLOGY

The retinal vasculature is composed of arteries and veins, with their tributaries visible within the retinal image. There is a wide range of vessel widths ranging from one pixel to 17 pixels, depending on both the width of the vessel and the image resolution. The vessels have a lower reflectance compared to other retinal surfaces, thus, they usually appear darker relative to the background. The central intensity of some vessels differs from the background by as little as four grey levels, and the background noise standard deviation is almost 2.3 grey levels [28]. A variety of structures appear in the images, including the retina boundary, the optic disc, and pathologies. The pathologies are particularly challenging to automatic vessel extraction because they may appear as a series of bright spots, sometimes with narrow, darker gaps in between. Light is absorbed and reflected by the retinal vessels, the retinal capillaries and the choroid. Variations in the thickness of the vessel wall and the index of refraction have negligible influence on the apparent width of the blood column. However, occasionally a light streak running the length of the vessel is reflected from the transparent convex wall of the arteriole [12]. Retinal vessels also exhibit a strong reflection along their centerline known as central vessel reflex, which is more pronounced in arteries than veins, and is stronger at longer wavelengths. This effect is believed to result from a specular reflection at the interface between the retina and vitreous, the internal limiting membrane. Light reflexes and artifactual features such as specular reflection are typically found in the retinal images of younger patients. However, the thickening and fibrosis of the vessel wall associated with arteriosclerosis changes the refractive index and increases the width of the light reflex. The anatomical structures in retinal images are shown in Figure 1.

The vessel cross-sectional intensity profiles approximate a Gaussian shape, or a mixture of Gaussians in case of central vessel reflex. The orientation and grey level of a vessel does not change abruptly; they are locally linear and gradually change in intensity along their lengths. The vessels can be expected to be connected and, in the retina, form a binary treelike structure. However, the shape, size and local grey level of blood vessels can vary hugely and some background features may have similar attributes to vessels. Vessel crossing and branching can further complicate the profile model. As with the processing of most medical images, signal noise, drift in image intensity and lack of image contrast pose significant challenges to the extraction of blood vessels.

There are some reviews [29, 30] available in the literature which give an overview of vessel segmentation techniques from 2-D as well as 3-D images in various application domains including (i) extraction of neurovascular structures (ii) retinal blood vessel segmentation, (iii) coronary artery extraction, (iv) extraction of blood vessels from mammograms, (v) human airway tree (pulmonary tree) segmentation, (vi) extraction of abdominal aorta and vascular structures in the legs, (vii) extraction of vascular structures in livers, (viii) colon extraction, (ix) segmentation of nerve channels and (x) extraction of tubular structures for industrial and

scientific applications. Other studies [30-33] present an overview of different algorithms for feature extraction, segmentation and registration of retinal images. The surveys [5, 34] [38,39] on algorithms for automatic detection of diabetic retinopathy are also presented.

3. RETINAL BLOOD VESSEL SEGMENTATION

3.1 Materials

The retinal vessel segmentation methodologies are evaluated on the publically available databases for retinal images. The datasets are discussed below.

3.1.1 DRIVE Database

The DRIVE (Digital Retinal Images for Vessel Extraction)[35] is a publically available database, consisting of a total of 40 color fundus photographs. The photographs were obtained from a diabetic retinopathy screening program in the Netherlands. The screening population consisted of 453 subjects between 31 to 86 years of age. Each image has been JPEG compressed, which is common practice in screening programs. Of the 40 images in the database, 7 contain pathology, namely exudates, hemorrhages and pigment epithelium changes. The images were acquired using a Canon CR5 non-mydriatic 3CCD camera with a 45 degree field of view (FOV). Each image is captured using 8 bits per color plane at 768 × 584 pixels. The FOV of each image is circular with a diameter of approximately 540 pixels. The set of 40 images was divided into a test and training set both containing 20 images. Three observers, the first and second author and a computer science student manually segmented a number of images. All observers were trained by an experienced ophthalmologist (the last author). The first observer segmented 14 images of the training set while the second observer segmented the other 6 images. The test set was segmented twice resulting in a set X and Y. Set X was segmented by both the first and second observer (13 and 7 images respectively) while set Y was completely segmented by the third observer. The performance of the vessel segmentation algorithms is measured on the test set. In set X the observers marked 577,649 pixels as vessel and 3,960,494 as background (12.7% vessel). In set Y 556,532 pixels are marked as vessel and 3,981,611 as background (12.3% vessel). Figure 2 shows the retinal images from DRIVE database.

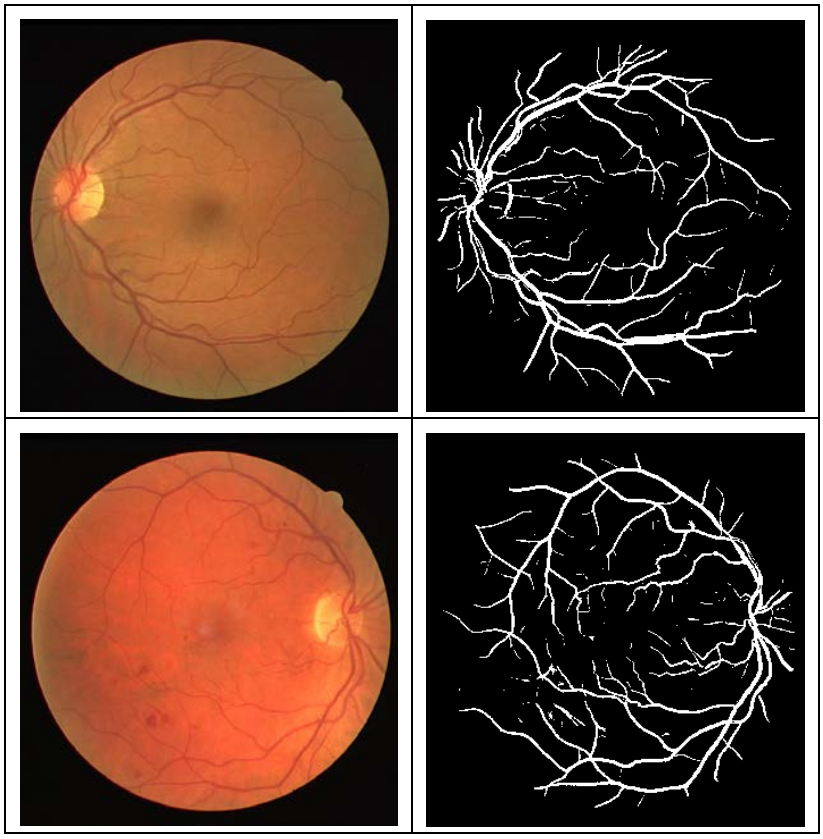

Figure 5: Retinal Images from DRIVE Database; (top row) Normal Image, (bottom row) Pathological Image. (a) Retinal image, (b) Segmented Vessels

3.1.2 STARE Database

The STARE database [36] contains 20 images for blood vessel segmentation; ten of these contain pathology. The digitized slides are captured by a TopCon TRV-50 fundus camera at 35^{o} field of view (FOV). The slides were digitized to 605 x 700 pixels, 8 bits per colour channel. The approximate diameter of the FOV is 650x500 pixels. Two observers manually segmented all the images. The first observer segmented 10.4% of pixels as vessel, against 14.9% vessels for the second observer. The segmentations of the two observers are fairly different in that the second observer segmented many more of the thinner vessels than the first one. Performance is computed with the segmentations of the first observer as the ground truth. Figure 3 illustrates the retinal images form STARE database.

Figure 6: Retinal Images from STARE Database; (top row) Normal Image, (bottom row) Pathological Image. (a) Retinal image, (b) Segmented Vessels

3.2 Performance Measures

In the retinal vessel segmentation process, the outcome is a pixel-based classification result. Any pixel is classified either as vessel or surrounding tissue. Consequently, there are four events; two classifications and two misclassifications.

3.2.1 Classifications

The classifications are

- True Positive (TP) ; when a pixel is correctly segmented as a vessel pixel i.e. the pixel is classified as a vessel pixel and it is actually the vessel pixel as per the gold standard (the manual segmentation by an expert)
- True Negative (TN); when a pixel is correctly segmented as a non-vessel, the pixel is classified as a non-vessel pixel and it is actually the non-vessel pixel as per the gold standard.

3.2.2 Mis-Classifications

The two misclassifications are

- False Negative (FN) occurs when a pixel in a vessel is segmented in the non-vessel area, i.e. the pixel is classified as non-vessel but actually it belongs to a vessel as per the gold standard.

- False Positive (FP) occurs when a non-vessel pixel is segmented as a vessel-pixel i.e. the pixel is actually the non-vessel pixel (as per the gold standard) but is classified as the vessel pixel.

The measures derived from the above events are

3.2.3 True Positive Rate

True Positive Rate (TPR) or true positive fraction represents the fraction of pixels correctly detected as vessel pixels. It is the ratio between the numbers of pixels correctly detected as vessel pixels to the count of pixels which are actually in vessels.

$$TPR = \frac{\text{\# of pixels correctly detected as vessel pixel}}{\text{\# of pixels actually in vessels}}$$

3.2.4 False Positive Rate

False Positive Rate (FPR) or false positive fraction represents the fraction of pixels erroneously detected as vessel pixels. It is obtained as the ration between the numbers of pixels erroneously detected as vessel pixels to the number of pixels which are actually in non-vessel region in the retinal image.

$$FPR = \frac{\text{\# of pixels erroneously detected as vessel pixel}}{\text{\# of pixels actually in non-vessels region}}$$

3.2.5 Accuracy

The accuracy is estimated by the ratio of the total number of correctly classified pixels (sum of true positives and true negatives) by the number of pixels in the image FOV.

$$Accuracy = \frac{\text{\# of correctly classified pixels}}{\text{\# of pixels in image FOV}}$$

3.2.6 Sensitivity

Sensitivity (SN) reflects the ability to detect vessel pixels. The sensitivity of a vessel detection algorithm is a measure of how well the algorithm performs in correctly identifying vessel pixels within a retinal fundus image.

Sensitivity is expressed as

$$SN = \frac{\text{TP}}{(\text{TP} + \text{FN})}$$

Where, TP and FN are the number of true positive and false negative results, respectively. Sensitivity can also be thought as 1- the False Negative Rate.

3.2.7 Specificity

Specificity (SP) is the ability to detect non-vessel pixels. The specificity of a vessel segmentation algorithm reflects how good the algorithm is correctly identifying the non-vessel pixels.

The formula for specificity is

$$SP = \frac{\mathrm{TN}}{(\mathrm{TN} + \mathrm{FP})}$$

Where, TN and FP are the number of true negative and false positive results, respectively. Specificity can also be written as,

$$SP = 1 - FPR$$

3.2.8 ROC Analysis

A receiver operating characteristic (ROC) curve plots the fraction of vessel pixels correctly classified as vessel, namely the true positive rate (TPR), versus the fraction of non-vessel pixels wrongly classified as vessel, namely the false positive rate (FPR). The closer the curve approaches the top left corner; the better is the performance of the system. The most frequently used performance measure extracted from the ROC curve is the value of the area under the curve (AUC) which is 1 for an optimal system. For retinal images, TPR and FPR are computed considering only pixels inside the FOV.

4. SUPERVISED METHODS FOR RETINAL VESSEL SEGMENTATION

Supervised methods exploit some prior labeling information to decide whether a pixel belongs to a vessel or not, while unsupervised methods perform the vessel segmentation without any prior labeling knowledge. In supervised methods, the rule for vessel extraction is "learned" by the algorithm on the basis of a training set of manually processed and segmented reference images often termed as "gold standard". This gold standard data set consists of a number of images whose vascular structure must be precisely marked by an ophthalmologist. However, as noted by Hoover et al. [37] there is significant disagreement in the identification of vessels even amongst expert observers. These methods classify individual pixels and require hand-labeled gold standard images for training. In a supervised method, the criteria are determined by the ground truth data based on given features. However, a prerequisite for a supervised method is the availability of the ground truth data that are already classified, which may not be available in real life applications. As supervised methods are designed based on pre-classified data, their performance is usually better than that of unsupervised ones and can produce very good results for healthy retinal images.

Artificial neural networks have been extensively investigated for segmenting retinal features such as the vasculature[38] making classifications based on statistical probabilities

rather than objective reasoning. These neural networks employ mathematical "weights" to decide the probability of input data belonging to a particular output. This weighting system can be adjusted by training the network with data of known output typically with a feedback mechanism to allow retraining.

Nekovei and Sun [39] describe an approach using a back-propagation network for the detection of blood vessels in X-ray angiography. The method applies the neural network directly to the angiogram pixels without prior feature detection. The pixels of the small sub-window which slides across the angiogram image, are directly fed as input to the network. The feature vectors are formed by gray-scale values from the sub window centered on the pixel being classified. The ground truth images of manually labeled angiograms are used as the training set to set the network's weights. A modified version of the common delta-rule is to obtain these weights. The proposed method does not extract the vascular structure but is to label the pixels as vessel or non-vessel.

Sinthanayothin et al. [40] preprocessed images with PCA to reduce background noise by reducing the dimensionality of the data set and then applied a neural network to identify the pathology. They reported a success rate of 99.56% for the training data and 96.88% for the validation data, respectively, with an overall sensitivity and specificity of 83.3% (standard deviation 16.8%) and 91% (standard deviation 5.2%), respectively. The result of the approach was compared with an experienced ophthalmologist manually mapping out the location of the blood vessels in a random sample of seventy three 20×20 pixel windows and requiring an exact match between pixels in both images.

Niemeijer et al. [41] extracts a feature vector for each pixel that consists of the Gaussian and its derivatives up to order 2 at scales s = 1, 2, 4, 8, 16 pixels, augmented with the green plane of the RGB image and then, uses a k-nearest neighbor (kNN) algorithm to estimate the probability of the pixel belonging to a vessel. Each feature is normalized to zero mean and unit variance before classification. By thresholding the probability map a binary segmentation of the vasculature can be obtained. The algorithm is tested on the DRIVE data set resulting in average accuracy of 0.9416 and area under the ROC curve of 0.9294

Staal et al. [42] presented a ridge based vessel segmentation methodology from colored images of the retina which exploits the intrinsic property that vessels are elongated structures. The technique is based on an extraction of image ridges, which are natural indicators of vessels and coincide approximately with vessel centerlines. Image primitives are computed by grouping the ridge pixels, therefore grouping the ridges to sets that approximate straight line elements. With these sets an image is partitioned into patches by assigning each image pixel to the closest line element. Every line element constitutes a local coordinate frame for its corresponding patch. Every line element defines a local coordinate frame termed as an affine convex set region within each patch, in which local features are extracted for every pixel. In total, 27 features are selected from convex set regions collectively as well as from individual pixels using

a sequential forward selection method. A K-NN classifier is used for classification. Some authors suggests [43] that by combining ridge features across multiple scales, the local vessel size is decoupled from the model. The methodology is tested on the publically available STARE [37] and Utrecht database obtained from a screening programme in the Netherlands. The method achieves an average accuracy of 0.9516 and an area under the ROC curve of 0.9614 on the STARE dataset.

The use of a 2-D gabor wavelet and supervised classification for retinal vessel segmentation has been demonstrated by Soares et al. [44]. Each pixel is represented by a feature vector composed of the pixel's intensity and two-dimensional Gabor wavelet transform responses taken at multiple scales. A Gaussian mixture model (a Bayesian classifier in which each class-conditional probability density function is described as a linear combination of Gaussian functions) classifier is used to classify each pixel as either a vessel or non-vessel pixel. The probability distributions are estimated based on a training set of labeled pixels obtained from manual segmentations. The methodology is evaluated on the DRIVE and STARE datasets resulting in average accuracy of 0.9466 & 0.9480 and the area under the ROC curve as 0.9614 & 0.9671 for DRIVE and STARE respectively. The algorithm takes in to account the information local to each pixel through image filters, ignoring useful information from shapes and structures present in the image. It does not work very well on the images with non-uniform illumination as it produces false detection in some images on the border of the optic disc, hemorrhages and other types of pathologies that present strong contrast.

Ricci et al. [45] proposed a methodology to segment retinal vessels using line operators and support vector classification. A line detector which is based on the evaluation of the average grey level along lines of fixed length passing through the target pixel at different orientations is applied to the green channel of an RGB image and the response is thresholded to obtain unsupervised pixel classification. Moreover, two orthogonal line detectors are also employed along with the grey level of the target pixel to construct a feature vector for supervised classification using a support vector machine. With respect to other supervised techniques, the algorithm 1) requires fewer features, 2) feature extraction is computationally simpler, and 3) fewer examples are needed for training. The algorithm makes use of local differential computation of the line strength which makes the line detector robust with respect to non-uniform illumination and contrast. Also the line detector behavior in the presence of a central reflex is quite satisfactory. The performance of both methods is evaluated on the publicly available DRIVE and STARE databases through ROC analysis, resulting in average accuracy of 0.9563 & 0.9584 and the area under ROC curve as 0.9558 & 0.9602 for DRIVE and STARE respectively.

Osareh and Shadgar [46] use multiscale Gabor filters for vessel candidate identification, then the features are extracted using principal component analysis. The parameters for Gabor filters are optimally tuned with experimentations. The image pixels are classified as vessels and

non-vessels using the corresponding feature vectors by Gaussian mixture model (GMM) and support vector machines (SVM). The methodology is tested on DRIVE as well as on the author's dataset consisting of 90 normal and abnormal images. The classification accuracy obtained is 95.24%, with 96.14% sensitivity and 94.84% specificity with GMM. The best overall accuracy, using optimal parameters for SVM is 96.75% with 96.50% sensitivity and 97.10% specificity. The methodology achieves area under the ROC curve as 0.965 on the DRIVE database. However, there are some false positives due to background noise and non-uniform illumination, the border of the optic disc and other types of pathologies and the thinnest vessels are also not detectable, however, these thin vessels are not of much clinical importance.

Salem et al [47] proposed a RAdius based Clustering ALgorithm (RACAL) which uses a distance based principle to map the distributions of the image pixels. A partial supervision strategy is combined with the clustering algorithm. The features used are the green channel intensity, the local maxima of the gradient magnitude, and the local maxima of the large eigenvalue calculated from Hessian matrix. The same features are used with kNN and RACAL algorithms and later perform better for the detection of small vessels. The methodology attains a specificity of 0.9750 and sensitivity of 0.8215 on the STARE database.

Xu and Luo [48] combines several image processing techniques with support vector machine(SVM) classification for vessel segmentation. In this methodology, the background of the green channel is normalized, the large vessels are segmented using adaptive local thresholding and the optic disk edges are removed. The original image is then processed by wavelets at multiple scales for feature extraction. The line detectors are used to identify thin vessels. A 12 dimensional feature vector for each residual pixel in the binary retinal image excluding large vessels is constructed and a support vector machine is used to distinguish thin vessel segments from all the fragments. A tracking method based on a combination of vessel direction and the eigenvector of the Hessian matrix is used for thin vessel growth to obtain a segmented vessel tree. The method achieves an average accuracy of 0.9328 and an average sensitivity of 0.7760 on the DRIVE database.

Lupascu et al. [49] introduces another supervised method known as feature-based AdaBoost classifier (FABC) for vessel segmentation. The 41-D feature vector is a rich collection of measurements at different spatial scales (√2, 2, 2√2 and 4), including the output of various filters (Gaussian and derivatives of Gaussian filters, matched filters, and 2-D Gabor wavelet transform), and the likelihood of structures like edges and ridges via numerical estimation of the differential properties of the intensity surface (principal and mean curvatures, principal directions, and root mean square gradient). This feature vector encodes a rich description of vessel-related image properties, namely local (pixel's intensity and Hessian-based measures), spatial (e.g., the gray-level profile of the cross section of a vessel can be approximated by a Gaussian curve) and structural (e.g., vessels are geometrical structures, which can be seen as tubular). An AdaBoost classifier is trained on 789,914 gold standard examples of vessel and

non-vessel pixels. The method achieves an average accuracy of 0.9597, an area under the ROC curve of 0.9561 and a kaapa measure of 0.72 on the DRIVE dataset. The strength of FABC lies in its capturing a rich collection of shape and structural information, in addition to local information at multiple spatial scales, in the feature vector. FABC does not discuss the issues related to the connection of broken vessel segments and some local ambiguities present due to the convergence of multiple and variously bent vessels.

The combination of the radial projection and the semi-supervised self-training method using SVM is employed by X. You [50] for vessel segmentation. The vessel centerlines and the narrow and low contrast blood vessels are located using radial projections. A modified steerable complex wavelet is employed for vessel enhancement. The line strength measures are applied to the vessel enhanced image to generate the feature vector. The SVM classifier is used in a semi-supervised self-training to extract the major structure of vessels. The segmented vasculature is obtained by the union of the two. The algorithm self learns from human-labeled data and weakly labeled data therefore yielding good results with decrease in the detection of false vessels. The method is very good in detecting narrow and low contrast vessels but prone to errors in case of pathologies. The average accuracy, sensitivity and specificity on the DRIVE database is 0.9434, 0.7410, and 0.9751 respectively and for the STARE database 0.9497, 0.7260, and 0.9756 respectively.

Marin [51] presented a neural network based supervised methodology for the segmentation of retinal vessels. The methodology uses a 7-D feature vector composed of gray-level and moment invariant-based features. A multilayer feed forward neural network is utilized for training and classification. The input layer consists of seven neurons, the three hidden layers consist of fifteen neurons each and output layer is comprised of single neuron. The method proves to be effective and robust with different image conditions and on multiple image databases even if the neural network is trained on only one database. The average accuracy, AUC, sensitivity and specificity on the DRIVE database is 0.9452, 0.9588, 0.7067, and 0.9801 respectively and for the STARE database 0.9526, 0.9769, 0.6944, and 0.9819 respectively.

Fraz et. al. [52] presented an effective retinal vessel segmentation technique based on supervised classification using an ensemble classifier of boosted and bagged decision trees. Their methodology has used a nine dimensional feature vector which consists of the vessel map obtained from the orientation analysis of the gradient vector field, the morphological transformation; line strength measures and the Gabor filter response which encodes information to successfully handle both normal and pathological retinal images. The important feature of bagged ensemble is that the reliable estimates of the classification accuracy and feature importance are obtained during the training process without supplying the test data. The ensemble classifier was constructed by using 200 weak learners and is trained on 200,000 training samples randomly extracted from the training set of the DRIVE and 75000 samples from STARE databases. These parameters are chosen by empirically analyzing the out-of-bag

classification for a given number of training samples and the decision trees. The average accuracy, AUC, sensitivity and specificity on the DRIVE database is 0.9480, 0.9747, 0.7406, and 0.9807 respectively and for the STARE database 0.9534, 0.9768, 0.7548, and 0.9763 respectively.

Table 1: Summary of supervised classification algorithms for vessel segmentation

Methodology	Database	Sensitivity	Specificity	Accuracy	Area under ROC
Human Observer	DRIVE	0.797	0.972	0.9473	-
	STARE	-	-	0.9354	-
Sinthanayothin	Local Dataset	0.833	0.91	-	-
Niemeijer	DRIVE	-	-	0.9416	0.9294
Staal	DRIVE	-	-	0.9442	0.952
	STARE	-	-	0.9516	0.9614
Soares	DRIVE	-	-	0.9466	0.9614
	SATRE	-	-	0.9480	0.9671
Ricci	DRIVE	-	-	0.9563	0.9558
	STARE	-	-	0.9584	0.9602
Osareh and Shadgar	DRIVE (SVM)	0.9650	0.9710	0.9675	0.974
	DRIVE(GMM)	0.9614	0.9484	0.9524	0.965
Salim	STARE	0.8215	0.9750	-	-
Lupascu	DRIVE	-	-	0.9597	0.9561
Xu and Luo	DRIVE	0.7760	-	0.9328(0.0075)	-
You et al., 2011 [50]	DRIVE	0.7410	0.9751	0.9434	
	STARE	0.7260	0.9756	0.9497	
Marin et al., 2011 [51]	DRIVE	0.7067	0.9801	0.9452	0.9588
	STARE	0.6944	0.9819	0.9526	0.9769
Fraz et al. [52]	DRIVE	0.7406	0.9807	0.9480	0.9747
	STARE	0.7548	0.9763	0.9534	0.9768

5. CONCLUSION

Retinal digital image analysis is able to exploit the ease with which the retinal circulation can be visualized, photographed, and analyzed non-invasively in vivo. Using objective, quantitative measures from retinal vasculature which are based on principals of optimization of a branching vasculature, studies have been able to improve our understanding of the effect of systemic factors on the microvasculature. The most commonly performed quantitative measurement from digital retinal vascular image analysis has

been the AVR. Whilst this has proved to be a very useful research tool to measure generalized arteriolar narrowing, very large epidemiological studies have been required to have sufficient statistical power to be able to detect associations of this entity with systemic factors. It is also unclear from current studies whether the detection of retinal microvascular changes has additional predictive value above current standardized methods. With an increasingly aged population and increased strain on medical resources, the use of strategies such as telemedicine and widespread screening of individuals at risk of certain diseases will increase. Retinal vascular digital image analysis will play an ever greater role in clinical ophthalmology.

REFERENCES

[1]. Abràmoff, M.D., M.K. Garvin, and M. Sonka, *Retinal Imaging and Image Analysis.* Biomedical Engineering, IEEE Reviews in, 2010. **3**: p. 169-208.

[2]. Kanski, J.J., *Clinical ophthalmology*. 6th edition ed2007, London: Elsevier Health Sciences (United Kingdom). 952.

[3]. Liang, Z., et al., *The detection and quantification of retinopathy using digital angiograms.* Medical Imaging, IEEE Transactions on, 1994. **13**(4): p. 619-626.

[4]. Teng, T., M. Lefley, and D. Claremont, *Progress towards automated diabetic ocular screening: A review of image analysis and intelligent systems for diabetic retinopathy.* Medical and Biological Engineering and Computing, 2002. **40**(1): p. 2-13.

[5]. Winder, R.J., et al., *Algorithms for digital image processing in diabetic retinopathy.* Computerized Medical Imaging and Graphics, 2009. **33**(8): p. 608-622.

[6]. Heneghan, C., et al., *Characterization of changes in blood vessel width and tortuosity in retinopathy of prematurity using image analysis.* Medical image analysis, 2002. **6**(4): p. 407-429.

[7]. Haddouche, A., et al., *Detection of the foveal avascular zone on retinal angiograms using Markov random fields.* Digital Signal Processing. **20**(1): p. 149-154.

[8]. Narasimha-Iyer, H., et al., *Automatic Identification of Retinal Arteries and Veins From Dual-Wavelength Images Using Structural and Functional Features.* Biomedical Engineering, IEEE Transactions on, 2007. **54**(8): p. 1427-1435.

[9]. Hatanaka, Y., et al. *Automated analysis of the distributions and geometries of blood vessels on retinal fundus images*. SPIE.

[10]. Foracchia, M., *Extraction and quantitative description of vessel features in hypertensive retinopathy fundus images*, in *Book Abstracts 2nd Int. Workshop on Computer Assisted Fundus Image Analysis*, E. Grisan, Editor 2001. p. 6-6.

[11]. Xiaohong, G., et al. *A method of vessel tracking for vessel diameter measurement on retinal images*. in *Image Processing, 2001. Proceedings. 2001 International Conference on*.

[12]. Lowell, J., et al., *Measurement of retinal vessel widths from fundus images based on 2-D modeling.* Medical Imaging, IEEE Transactions on, 2004. **23**(10): p. 1196-1204.

[13]. Hong, S., et al., *Optimal scheduling of tracing computations for real-time vascular landmark extraction from retinal fundus images.* Information Technology in Biomedicine, IEEE Transactions on, 2001. **5**(1): p. 77-91.

[14]. Pinz, A., et al., *Mapping the human retina.* Medical Imaging, IEEE Transactions on, 1998. **17**(4): p. 606-619.

[15]. Zana, F. and J.C. Klein, *A multimodal registration algorithm of eye fundus images using vessels detection and Hough transform.* Medical Imaging, IEEE Transactions on, 1999. **18**(5): p. 419-428.

[16]. Can, A., et al., *A Feature-Based, Robust, Hierarchical Algorithm for Registering Pairs of Images of the Curved Human Retina.* IEEE Transactions on Pattern Analysis and Machine Intelligence, 2002. **24**: p. 347-364.

[17]. Fritzsche, K., et al., *Automated Model Based Segmentation, Tracing and Analysis of Retinal Vasculature from Digital Fundus Images*, in *State-of-The-Art Angiography, Applications and Plaque Imaging Using MR, CT, Ultrasound and X-rays*2003, Academic Press. p. 225-298.

[18]. Hoover, A. and M. Goldbaum, *Locating the optic nerve in a retinal image using the fuzzy convergence of the blood vessels.* Medical Imaging, IEEE Transactions on, 2003. **22**(8): p. 951-958.

[19]. Foracchia, M., E. Grisan, and A. Ruggeri, *Detection of optic disc in retinal images by means of a geometrical model of vessel structure.* Medical Imaging, IEEE Transactions on, 2004. **23**(10): p. 1189-1195.

[20]. Huiqi, L. and O. Chutatape, *Automated feature extraction in color retinal images by a model based approach.* Biomedical Engineering, IEEE Transactions on, 2004. **51**(2): p. 246-254.

[21]. Fritzsche, K.H., *Computer vision algorithms for retinal vessel detection and width change detection*, 2004, Rensselaer Polytechnic Institute: Troy, NY, USA.

[22]. Houben, A.J.H.M., et al., *Quantitative analysis of retinal vascular changes in essential and renovascular hypertension.* Journal of hypertension, 1995. **13**(12).

[23]. Wasan, B., et al., *Vascular network changes in the retina with age and hypertension.* Journal of hypertension, 1995. **13**(12).

[24]. Koozekanani, D., et al., *Tracking the Optic Nerve Head in OCT Video Using Dual Eigenspaces and an Adaptive Vascular Distribution Model.* Computer Vision and Pattern Recognition, IEEE Computer Society Conference on, 2001. **1**: p. 934.

[25]. Solouma, N.H., et al., *A new real-time retinal tracking system for image-guided laser treatment.* Biomedical Engineering, IEEE Transactions on, 2002. **49**(9): p. 1059-1067.

[26]. Mari, et al., *Personal authentication using digital retinal images.* Pattern Anal.Appl., 2006. **9**(1): p. 21-33.

[27]. Chia-ling, T., et al., *Model-based method for improving the accuracy and repeatability of estimating vascular bifurcations and crossovers from retinal fundus images*, 2004.

[28]. Sofka, M. and C.V. Stewart, *Retinal Vessel Centerline Extraction Using Multiscale Matched Filters, Confidence and Edge Measures.* Medical Imaging, IEEE Transactions on, 2006. **25**(12): p. 1531-1546.

[29]. Kirbas, C. and F. Quek, *A review of vessel extraction techniques and algorithms.* ACM Comput.Surv., 2004. **36**(2): p. 81-121.

[30]. Fraz, M.M., et al., *Blood vessel segmentation methodologies in retinal images – A survey.* Computer methods and programs in biomedicine, 2012. **108**(1): p. 407-433.

[31]. Mabrouk, M.S., N.H. Solouma, and Y.M. Kadah, *Survey of Retinal Image Segmentation and Registration.* ICGST International Journal on Graphics, Vision and Image Processing, 2006. **6**(2): p. 1-11}.

[32]. Patton, N., et al., *Retinal image analysis: Concepts, applications and potential.* Progress in retinal and eye research, 2006. **25**(1): p. 99-127.

[33]. Stewart, C., et al., *Computer Vision Algorithms for Retinal Image Analysis: Current Results and Future Directions*, in *Computer Vision for Biomedical Image Applications*2005, Springer Berlin / Heidelberg. p. 31-50.

[34]. Faust, O., et al., *Algorithms for the Automated Detection of Diabetic Retinopathy Using Digital Fundus Images: A Review.* Journal of medical systems: p. 1-13.

[35]. Niemeijer, M., et al., *DRIVE: Digital Retinal Images for Vessel Extraction*, 2004.

[36]. *STARE: STructured Analysis of the Retina, http://www.ces.clemson.edu/~ahoover/stare/*. 2000.

[37]. Hoover, A.D., V. Kouznetsova, and M. Goldbaum, *Locating blood vessels in retinal images by piecewise threshold probing of a matched filter response.* Medical Imaging, IEEE Transactions on, 2000. **19**(3): p. 203-210.

[38]. Akita, K. and H. Kuga, *A computer method of understanding ocular fundus images.* Pattern Recognition, 1982. **15**(6): p. 431-443.

[39]. Nekovei, R. and S. Ying, *Back-propagation network and its configuration for blood vessel detection in angiograms.* Neural Networks, IEEE Transactions on, 1995. **6**(1): p. 64-72.

[40]. Sinthanayothin, C., et al., *Automated localisation of the optic disc, fovea, and retinal blood vessels from digital colour fundus images.* British Journal of Ophthalmology, 1999. **83**(8): p. 902-910.

[41]. Abramoff, M.N., et al. *Comparative study of retinal vessel segmentation methods on a new publicly available database*. in *SPIE Medical Imaging*. 2004. SPIE.

[42]. Staal, J., et al., *Ridge-based vessel segmentation in color images of the retina.* Medical Imaging, IEEE Transactions on, 2004. **23**(4): p. 501-509.

[43]. Li, W., A. Bhalerao, and R. Wilson, *Analysis of Retinal Vasculature Using a Multiresolution Hermite Model.* Medical Imaging, IEEE Transactions on, 2007. **26**(2): p. 137-152.

[44]. Soares, J.V.B., et al., *Retinal vessel segmentation using the 2-D Gabor wavelet and supervised classification.* Medical Imaging, IEEE Transactions on, 2006. **25**(9): p. 1214-1222.

[45]. Ricci, E. and R. Perfetti, *Retinal Blood Vessel Segmentation Using Line Operators and Support Vector Classification.* Medical Imaging, IEEE Transactions on, 2007. **26**(10): p. 1357-1365.

[46]. Osareh, A. and B. Shadgar, *Automatic Blood Vessel Segmentation In Color Images Of Retina.* Iranian Journal Of Science And Technology Transaction B-Engineering, 2009. **33**(B2): p. 191-206.

[47]. Salem, S., N. Salem, and A. Nandi, *Segmentation of retinal blood vessels using a novel clustering algorithm (RACAL) with a partial supervision strategy.* Medical and Biological Engineering and Computing, 2007. **45**(3): p. 261-273.

[48]. Xu, L. and S. Luo, *A novel method for blood vessel detection from retinal images.* BioMedical Engineering OnLine, 2010. **9**(1): p. 14.

[49]. Lupascu, C., et al., *A Comparative Study on Feature Selection for Retinal Vessel Segmentation Using FABC*, in *Computer Analysis of Images and Patterns*2009, Springer Berlin / Heidelberg. p. 655-662.

[50]. You, X., et al., Segmentation of retinal blood vessels using the radial projection and semi-supervised approach. Pattern Recognition, Volume 44, Issues 10–11, Pages 2314–2324

[51]. Marin, D., et al., *A New Supervised Method for Blood Vessel Segmentation in Retinal Images by Using Gray-Level and Moment Invariants-Based Features.* Medical Imaging, IEEE Transactions on, 2011. **30**(1): p. 146-158.

[52]. Fraz, M.M., et al., *An Ensemble Classification-Based Approach Applied to Retinal Blood Vessel Segmentation.* Biomedical Engineering, IEEE Transactions on, 2012. **59**(9): p. 2538-2548.